Structural Behaviour of Slender Columns of High Strength S690 Steel Welded H-Sections under Axial Compression

Tian-Yu Ma[1,2], Xiao Liu[2,3], Yi-Fei Hu[2,3], Kwok-Fai Chung[2,3] and Guo-Qiang Li[1]

[1] *College of Civil Engineering, Tongji University, Shanghai, China.*

[2] *Department of Civil and Environmental Engineering, the Hong Kong Polytechnic University, Hong Kong SAR, China.*

[3] *Chinese National Engineering Research Centre for Steel Construction (Hong Kong Branch), Hong Kong SAR, China.*

Abstract: This paper presents an experimental investigation into structural behaviour of slender columns of high strength S690 steel welded H-sections under axial compression. A total of seven slender columns with four sections of different cross-sectional dimensions and two different effective lengths were tested successfully. As expected, all of these columns failed in overall buckling about minor axes of their cross-sections, similar to those of conventional steel welded H-sections. Hence, these tests may be regarded to be confirmatory tests to structural behaviour of slender columns of high strength S690 steel welded H-sections under axial compression. No welding failure was observed after close inspection to all the columns after tests.

It should be noted that the measured failure loads of these slender columns were directly compared with predicted resistances of corresponding sections based on their measured geometrical and materials properties according to current design rules given in European, Chinese, and American Steel Codes, namely, EN 1993-1-1, GB 50017-2003, and ANSI/AISC 360-16 respectively. As effects of residual stresses in S690 steel welded H-sections were considered to be proportionally less pronounced when compared with those in S355 steel welded H-sections, their buckling resistances should be significantly increased when compared with those S355 welded H-sections. It was found that the current design rules given in both EN 1993-1-1 and GB 50017-2003 underestimated buckling resistances of slender columns of S690 steel welded H-sections significantly, and use of a different buckling curve with an increased structural efficiency was suggested. However, the predicted resistances of these slender columns to the current design rules given in ANSI/AISC 360-16 were found to be close to the measured failure loads. Hence, they were considered to be ~~directly~~ applicable to design slender columns of S690 steel welded H-sections.

Keywords: **High strength steel; Welded H-sections; Compression; Experiment; Design**

1 Introduction

With advancement of steel production technology in the past two decades, structural steel materials with high yield strengths and ductility have been available to construction. Those steel materials with yield strengths higher than 460 N/mm^2 are currently referred as high strength steel materials. High strength steel materials are widely considered to be able to give efficient structural solutions in heavily load members, such as columns in high-rise buildings and beam-column frames with long spanning beams[1] [2] [3] [4]. Compared with conventional steel materials, high strength steel materials possess excellent strength to self-weight ratios, reduced tensile to yield strength ratios, and reduced elongations at fracture. These characteristics will influence behaviour of structural steel members made of high strength steel materials. Effects of both material and geometrical initial imperfections onto structural stability of S690 steel sections should be quantified.

Initial material imperfection in the form of residual stresses is generally considered to be one of the major factors affecting structural stability of slender columns of S690 steel welded H-sections. According to previous studies on residual stresses in various welded sections made of high strength steel plates [5] [6] [7] [8] [9] [10] [11] [12] [13] [14], it was found that the magnitudes of welding induced residual stresses were generally independent from the yield strengths of the steel plates. Thus, the ratios of maximum residual stresses to yield strengths of high strength steel plates were significantly smaller than those of welded sections made of conventional steel materials. Consequently, it is expected that members made of high strength steel plates will give higher buckling resistances than those made of conventional steel plates on a proportional basis.

Structural behavior of welded sections made of high strength steel plates has been investigated by many researchers in the past two decades. Rasmussen and Hancock [5] measured compressive resistances of stocky columns made of S690 steel plates, and concluded that the plate slenderness limits obtained from welded sections of conventional steel plates were applicable to those welded sections made of high strength steel plates. However, Yuan [15] compared deformation capacities of stocky columns made of steel materials with different steel grades. However, he considered that the classification limits obtained from sections of conventional steel plates could not guarantee sufficient deformation capacities to be mobilized in sections made up of high strength steel plates.

Axial buckling behaviour of welded sections made of high strength steel plates was also examined by Rasmussen and Hancock [6], Li et. al [16], and Ban et al. [17], and it should be noted that these H-sections buckled about minor axes of their cross-sections. With the use of substantial restraining beams and bracings, a series of high strength

S690 steel welded H-sections were conducted by Shi et al. [18]. In these tests, all the columns were restrained with beams at both ends while out-of-plane and torsional deformations of the columns were restrained with braces. All of these columns were found to buckle about major axes of their cross-sections, and failed at buckling resistances significantly larger than those design values[6] [16] [17] [18]. Such improvement was attributed to reduced effects from both residual stresses and initial geometrical out-of-straightness. It should be noted that for those sections made of S460 steel materials, improvement on axial buckling resistances of these sections was found to be not as significant as those made of S690 and S960 steel materials [19] [20] [21] [22] .

Currently, EN 1993-1-1 [23] provides a design method for columns of S235 to S460 steel welded H-sections. To extend the design method to welded H-sections of high strength steels, EN 1993-1-12 [24] gives supplementary rules for up to S700 steel sections. Moreover, ANSI/AISC 360-16 [25] covers up to S690 steel sections (ASTM A514 and A709 steel sections) while GB 50017-2003 [26] is only applicable to S235 to S420 steel sections. As development of these design codes was based on experimental results conducted with conventional steel materials, there is a concern on applicability of these codes in designing high strength steel sections [6] [16] [17] [18].

1.1 Objectives and the scope of work

In order to promote an effective use of high strength steel sections in building construction, a comprehensive research programme was undertaken to investigate structural behaviour of beams and columns made of S690 steel welded H-sections, and to establish supplementary design rules through calibration against test results. As effects of residual stresses in S690 steel welded H-sections were considered to be proportionally less pronounced when compared with those in S355 steel welded H-sections, their buckling resistances should be significantly increased, when compared with those S355 steel welded H-sections.

This paper presents an experimental investigation into structural behaviour of slender columns of high strength S690 steel welded H-sections under axial compression. A total of seven slender columns with four sections of different cross-sectional dimensions and two different effective lengths were tested under axial compression. All of them were designed to undergo overall flexural buckling about minor axes of their cross-sections. Standard tensile tests were also carried out on coupons cut from S690 steel plates of various thickness to establish their mechanical properties. After testing, the measured failure loads of these slender columns would be directly compared with predicted resistances of corresponding sections based on their measured geometrical and material properties according to various design rules given in European, Chinese and American Steel Codes.

It should be noted that these high strength S690 steel welded H-sections are expected to behave in various ways similar to those of welded H-sections made of conventional steel materials. Hence, these tests may be regarded to be confirmatory tests to structural behaviour of S690 steel welded H-sections under axial compression. It is highly desirable to establish applicability of current design rules given in various codes for high strength S690 steel welded H-sections under axial compression through calibration against test results.

Furthermore, there was a complementary experimental investigation into structural behaviour of high strength S690 steel welded H-sections under combined compression and bending [27]. A total of eight slender columns with four sections of different cross-sectional dimensions and two different effective lengths were tested successfully under eccentric loads. Applicability of current design rules given in various codes has also been established with properly selected parameters through calibration against test results.

2 Experimental Investigation

2.1 Overview of test programme

A total of seven slender columns of S690 steel welded H-sections were tested under axial compression. These columns were made from S690 high strength steel plates in quenched and tempered condition with nominal thicknesses of 6, 10 and 16 mm. Four sections of different cross-sectional dimensions, namely, Sections H1, H2, H3 and H4 were adopted, and their nominal cross-sectional dimensions are shown in Figure 1.

It should be noted that:

a) For Section H1, only a column with a length of 1610 mm was tested.
b) For each of Sections H2, H3 and H4, a column with a length of 1610 mm and a column with a length of 2410 mm were tested.

Table 1 summarizes measured dimensions of the columns. It should be noted that these columns were devised in such a way that their slenderness ratios ranged from 0.6 to 1.4, i.e. within the range of intermediate slenderness.

2.2 Fabrication of welded H-sections

All the steel plates were cut using plasma cutting. Before welding, the steel plates were tack-welded to form H-sections, and a preheating of 120 °C was applied to the web-to-flange connections to reduce risks of hydrogen induced cracking.

For each column, the web was connected to the flanges by fillet welds on both sides. Gas metal arc welding (GMAW) with a fillet leg size of 6 mm was used for Sections H1 and H2 while submerged arc welding (SAW) with a fillet leg size of 10 mm was

used for Sections H3 and H4. Each fillet was completed by a single welding pass. It should be noted that as the electricity parameters fluctuated within a small margin during welding, average values of various welding parameters are presented in Table 2 together with materials specifications of welding electrodes. SAW was done with an automatic welding machine by a qualified welding operator while GMAW was done by a qualified welder. After the column was assembled, a pair of 30 mm thick S355 steel plates were groove welded onto both ends of the column.

2.3 Standard tensile tests

In order to establish material properties of S690 steel plates, nine coupons were machined from steel plates with nominal thicknesses of 6, 10 and 16 mm. Tensile tests on carefully machined coupons of these steel plates were carried out in accordance with EN ISO 6892-1 [28]. Two strain gauges were attached at the mid-section of each coupon to measure strains in the initial deformation range while digital imaging technique was employed to measure strains in the large deformation range. Deformations of the coupons at various loading stages were recorded by a digital camera, and elongations of the coupons were analysed through reading numbers of pixels in the digital images.

All the standard tensile tests were conducted on a MTS Testing Machine with a force capacity of 50 kN at a deformation rate of 0.25 to 0.3 mm per minute. The tensile tests were paused 3 times, each for 60 seconds after first yielding of the coupons in order to obtain lower bound values of the yield strengths, and the stress-strain curves of all the coupons are plotted onto the same graph for direct comparison as shown in Figure 2. It is shown that there is a definite yield plateau in each of these measured curves for various steel plates. Table 3 summarizes various measured material properties of these steel plates. It should be noted that in EN 1993-1-12, for S460 to S700 steel materials, the following ductility requirements are specified: i) $f_u / f_y \geq 1.05$; ii) elongation at failure not less than 10 %; and iii) $\varepsilon_u \geq 15\, f_y / E$. It is shown that all the steel plates employed in the present study satisfy these ductility requirements.

2.4 Test set-up and procedures

Before testing, the initial out-of-straightness of each column was measured. As shown in Figure 3, a steel wire was tightened on the top surface of one flange of the column, and it ran through the middle of the flange from one end of the column to the other end. Any deviation of the mid-width of the flange at the mid-length was regarded as the initial out-of-straightness of this flange, and it is denoted as v_1. This measurement was repeated on the other flange to obtain another initial out-of-straightness, v_2. The average value of v_1 and v_2 was considered to be the initial out-of-straightness of the column, v, and all of these measurements are presented in Table 4. Due to limitations of the measurement method, any value smaller than 0.25 mm, that is the radius of the steel wire, cannot be identified, and this situation is denoted with "--". It is shown that the

absolute values of the measured initial out-of-straightness of all the columns are smaller than L_{eff} / 1000.

All the tests were conducted with a 1,000 tons Universal Servo Controlled Testing Machine, and the test set-up is shown in Figure 4. In each test, a pair of attachments were connected to both ends of the column through bolts, and these attachments enabled free rotations of the column ends about minor axes of the cross-sections. It should be noted that the ends of the attachment were carefully milled into semi-cylinders with a diameter of 50mm, and they were expected to rotate freely in a matching semi-cylindrical groove with the same diameter. As grease was applied onto the contact surfaces before testing, friction between these surfaces was eliminated as much as practically possible. Typical arrangement of strain gauges and displacement transducers is shown in Figure 5. A total of twelve strain gauges were mounted onto the outer surfaces of the flanges at three cross-sections of the column, namely, Sections A-A, B-B and C-C. At each section, four strain gauges were installed 10 mm away from the flange tips. Displacement transducers DT 1 and DT2 were used to record lateral deflections of the column at Section B-B in the direction of the major axis of the cross-section. Any difference in the measurements between Transducers DT1 and DT2 gave a twisting of the column. Transducer DT 3 was used to capture any lateral deflection of the column along the minor axis at Section B-B while Transducer DT 4 was used to measure axial deformation of the column.

For each test, the load was applied at a loading rate of 50 kN/min, and this rate was maintained until 80% of the predicted resistance was reached. Then, a displacement control was applied with a rate of 0.2 to 0.5 mm/min. The test would be terminated when the applied load dropped significantly, and the maximum applied load was taken as the failure load of the column.

2.5 Test results

All the columns were tested successfully, and all of them failed by overall buckling about the minor axes of their cross-sections. End rotations of all the columns were apparent while local plate buckling only took place in Test CH4P. Typical failure mode is shown in Figure 6, and the failure loads of all the columns are summarized in Table 5. Moreover, the applied load versus axial deformation curves for all the columns are shown in Figure 7. It should be noted that in all cases, the applied loads increased linearly with an increase of the axial deformations, and decreased sharply after the failure loads were attained. Moreover, the applied load versus lateral deflection curves of all the columns are shown in Figure 8. It was evident that in all cases, the columns began to deflect shortly after the axial loads were applied, and the lateral deflections increased gradually and linearly with an increase of the applied loads. As the applied loads approached the failure loads, lateral deflections of the columns developed quickly together with a sudden drop in the applied loads.

The applied load versus longitudinal strain curves at mid-height of all the columns are shown in Figure 9. In each graph. the curves coincide with each other well at the initial stage, and this indicates uniform compression. However, as the applied load increases, these curves begin to separate when the lateral deflection of the column becomes significant. It is evident that when the applied load approaches the failure load, compressive strains measured at the flanges are close to or even well exceed the value of f_y / E, and this signifies that the column fails with significant yielding.

For detailed information of measured residual stresses of these welded sections, refer to Reference 29.

3 Applicability of Codified Design Rules

In order to verify applicability of various codified design rules to design slender columns of S690 steel welded H-sections, all the test data and the measured failure loads of the slender columns reported above will be adopted to calibrate against relevant design rules given in EN 1993-1-1, GB 50017-2003, and ANSI/AISC 360-16. It should be noted that, in both EN 1993-1-1 and GB 50017-2003, multiple curves are available to evaluate member resistances, depending on steel grades, fabrication procedures, section types, plate thicknesses and axes of buckling. These curves differentiate among each other with the use of different imperfection parameters. However, in ANSI/AISC 360-16, only one buckling curve is given.

3.1 EN 1993-1-1

The design formula for column buckling is given in Cl.6.3.1 of EN 1993-1-1, and it follows the format of Aryton-Perry formula. A generalized initial imperfection parameter, η, is employed to incorporate effects of initial imperfections such as residual stresses, initial out-of-straightness and nominal loading eccentricities. It should be noted that η is expressed as

$$\eta = \alpha\left(\bar{\lambda} - \bar{\lambda}_0\right) \tag{1}$$

where α is an imperfection factor, and it depends on cross-sectional shape, buckling plane, plate thickness, and buckling axes; $\bar{\lambda}$ is a non-dimensional slenderness of the column under consideration; and $\bar{\lambda}_0$ is a parameter to define the length of the plateau along which the strength reduction resulted from overall flexural buckling is insignificant. Table 6 summarizes values of the imperfection factors for buckling design given in EN 1993-1-1.

The scope of application of EN 1993-1-1 is extended up to S700 steel materials with supplementary rules given in EN 1993-1-12. Hence, for design of slender columns of

S690 steel welded H-sections to be buckled about minor axis, buckling curve c should be used as recommended in Cl.6.2.3 of EN 1993-1-12. Figure 10 plots these buckling curves together with the measured resistances for direct comparison. It is shown that all the test data lie significantly above buckling curve c, and even above buckling curve a_0. This shows that the current design method underestimates the member resistances of these S690 steel welded H-sections considerably. It should be noted that the test result of Test CH2P is very high, and it lies close to the elastic buckling curve. A comparison between the measured and the predicted resistances of the columns are presented in Table 7. The ratios of the measured to the predicted resistances using buckling curve c, $\chi_t/\chi_{EC3,c}$, are shown to range from 1.22 to 1.49 while the ratios of the measured to the predicted resistances using buckling curve a_0, $\chi_t/\chi_{EC3,a0}$, are shown to range merely from 1.02 to 1.18. Hence, buckling curve a_0 may be safely adopted for design of slender columns of S690 steel welded H-sections.

3.2 Design to GB50017-2003

In GB 50017-2003, the buckling curves are determined by a set of imperfection factors, α_1, α_2 and α_3, which depend on cross-sectional shape, buckling axis, etc. When $\overline{\lambda} \leq 0.215$, the reduction factor, χ, is given by

$$\chi = 1 - \alpha_1 \overline{\lambda}^2 \tag{2}$$

When $\overline{\lambda} > 0.215$, the formula for the reduction factor follows the format of Aryton-Perry formula. A generalized initial imperfection factor, η, is employed to estimate effects of initial imperfections such as residual stresses, initial out-of-straightness and nominal loading eccentricities. However, being different from EN 1993-1-1, η is given by:

$$\eta = (\alpha_2 - 1) + \alpha_3 \overline{\lambda} \tag{3}$$

There are a total of four buckling curves, and the corresponding imperfection factors are presented in Table 8. It should be noted that GB50017 is not intended to be used to design S690 steel welded H-sections.

Figure 11 plots the measured resistances together with various buckling curves given in GB 50017 for direct comparison. It is shown that all the measured resistances are well above buckling curve b, and even buckling curve a. Comparison between the measured and the predicted resistances using buckling curves b and a are summarized in Table 9. Except Test CH2P, the ratios of the measured to the predicted resistances using buckling curve b, $\chi_t/\chi_{GB,b}$ are found to be significantly larger than unity, ranging from 1.15 to 1.36, while the ratios of the measured to the predicted resistances using buckling curve a, $\chi_t/\chi_{GB,a}$, are found to be moderately larger than unity, ranging from

1.07 to 1.22. Hence, buckling curve a may be safely adopted for design of slender columns of S690 steel welded H-sections.

3.3 Design to ANSI/AISC 360-16

It should be noted that ANSI/AISC 360-16 is generally applicable up to S690 steel sections, and there is only one buckling curve for designing of all columns. This buckling curve is based on the numerical results using an initial out-of-straightness of $L_{eff}/1500$. The reduction factor, χ, is given by

$$\chi = \begin{cases} 0.658\exp\left(\overline{\lambda}^2\right) & \text{for } 0 \le \overline{\lambda} \le 1.5 \\ 0.877\left(\frac{1}{\overline{\lambda}^2}\right) & \text{for } \overline{\lambda} \ge 1.5 \end{cases} \quad (4)$$

Figure 12 plots the measured resistances together with the buckling curve in ANSI for direct comparison, and it is shown that all the measured resistances lie above the buckling curve. Comparison between the measured and the predicted resistances is summarized in Table 10, and the ratios of the measured to the predicted resistances are found to be moderately larger than unity, ranging from 1.08 to 1.18. Therefore, this buckling curve is considered to be ~~readily~~ applicable to design of slender columns of S690 steel welded H-sections.

4 Conclusions

A total of seven slender columns of high strength S690 steel welded H-sections were tested successfully under axial compression. As expected, these columns were demonstrated to behave essentially similar to those welded H-sections made of conventional steel materials. All of them failed in overall buckling about minor axes of their cross-sections. Hence, these tests may be regarded to be confirmatory tests to structural behavior of high strength S690 steel welded H-sections under axial compression.

All the measured failure loads were compared with the predicted resistances of these slender columns according to current design rules given in EN 1993-1-1, GB 50017-2003 and ANSI/AISC 360-16. As effects of residual stresses in S690 steel welded H-sections were considered to be proportionally less pronounced when compared with those in S355 steel welded H-sections, their buckling resistances should be significantly increased when compared with those S355 steel welded H-sections. It was found that the current design rules in both EN 1993-1-1 and GB 50017-2003 underestimated buckling resistances of slender columns of S690 steel welded H-sections significantly, and use of a different buckling curve with an increased structural efficiency was suggested. However, the predicted resistances of these slender columns to the current

design rules in ANSI/AISC 360-16 were found to be close to the measured failure loads, and hence, they were considered to be ~~directly~~ applicable to design slender columns of S690 steel welded H-sections.

Consequently, the experimental investigation presented in this paper together with that presented in Reference 27 will provide physical evidence and confirmatory test data for establishment of supplementary design rules for S690 steel welded H-sections.

Acknowledgement

The authors are grateful to the financial support provided by the National Natural Science Foundation of China (Granted Project No. 51378378) and the Research Grant Council of the Government of Hong Kong SAR (Project No. PolyU 152194/15E). The project leading to the publication of this paper is also partially funded by the Research Committee (Project Nos. 4-9A6X, RTZX and RTK3) and the Chinese National Engineering Research Centre for Steel Construction (Hong Kong Branch) (Project No. 1-BBY3 & 4) of the Hong Kong Polytechnic University. The research studentships of the first three authors provided by the Tongji University and the Hong Kong Polytechnic University are acknowledged. Special thanks go to the Nanjing Iron and Steel Company Ltd. in Nanjing, the Zhongyi Steel Structure Co. Ltd. in Zhongshan and the Program Contractors Ltd. in Zhuhai. Thanks also go to the Hong Kong Constructional Metal Structures Association and the Macau Society of Metal Structures for their assistance in the fabrication of all the test specimens. All structural tests on high strength S690 steel welded H-sections were carried out at the Structural Engineering Research Laboratory of the Department of Civil and Environmental Engineering at the Hong Kong Polytechnic University, and supports from the technicians are gratefully acknowledged.

Reference

[1] Y. J. Shi, 'Recent Developments on High Performance Steel for Buildings', *Adv. Struct. Eng.*, vol. 15, no. 9, pp. 1617–1622, 2012.

[2] B. Johansson and P. Collin, 'Eurocode for high strength steel and applications in construction', in *Proceedings 'Super-High Strength Steels': 1st international conference*, 2005.

[3] C. Miki, K. Homma, and T. Tominaga, 'High strength and high performance steels and their use in bridge structures', *J. Constr. Steel Res.*, vol. 58, no. 1, pp. 3–20, 2002.

[4] R. Willms, 'High strength steel for steel constructions', in *Nordic steel construction conference*, 2009, pp. 597–604.

[5] K. J. R. Rasmussen and G. J. Hancock, 'Plate slenderness limits for high strength steel sections', *J. Constr. Steel Res.*, vol. 23, pp. 73–96, 1992.

[6] K. J. R. Rasmussen and G. J. Hancock, ‘Tests of high strength steel columns’, *J. Constr. Steel Res.*, vol. 34, no. 1, pp. 27–52, 1995.
[7] Y. B. Wang, G. Q. Li, and S. W. Chen, ‘Residual stresses in welded flame-cut high strength steel H-sections’, *J. Constr. Steel Res.*, vol. 76, pp. 159–165, 2012.
[8] Y. B. Wang, G. Q. Li, and S. W. Chen, ‘The assessment of residual stresses in welded high strength steel box sections’, *J. Constr. Steel Res.*, vol. 76, pp. 93–99, 2012.
[9] H. Y. Ban, G. Shi, Y. J. Shi, and Y. Q. Wang, ‘Residual stress of 460MPa high strength steel welded box section: Experimental investigation and modeling’, *Thin-Walled Struct.*, vol. 64, pp. 73–82, 2013.
[10] D. K. Kim, C. H. Lee, K. H. Han, J. H. Kim, S. E. Lee, and H. B. Sim, ‘Strength and residual stress evaluation of stub columns fabricated from 800MPa high-strength steel’, *J. Constr. Steel Res.*, vol. 102, pp. 111–120, Nov. 2014.
[11] B. Uy, ‘Strength of short concrete filled high strength steel box columns’, *J. Constr. Steel Res.*, vol. 57, no. 2, pp. 113–134, 2001.
[12] D. Beg and L. Hladnik, ‘Slenderness limit of class 3 I cross-sections made of high strength steel’, *J. Constr. Steel Res.*, vol. 38, no. 3, pp. 201–217, 1996.
[13] N. Tebedge and L. Tall, ‘Residual stresses in structural steel shapes-a summary of measured values. Fritz Laboratory Reports. Paper 350.’, Bethlehem, 1973.
[14] T. J. Li, G. Q. Li, and Y. B. Wang, ‘Residual stress tests of welded Q690 high-strength steel box- and H-sections’, *J. Constr. Steel Res.*, vol. 115, pp. 283–289, 2015.
[15] B. Yuan, ‘Local Buckling of High Strength Steel W-Shaped Sections’, McMaster University, 1997.
[16] T. J. Li, G. Q. Li, S. L. Chan, and Y. B. Wang, ‘Behavior of Q690 high-strength steel columns: Part 1: Experimental investigation’, *J. Constr. Steel Res.*, vol. 123, pp. 18–30, 2016.
[17] H. Y. Ban, G. Shi, Y. J. Shi, and M. A. Bradford, ‘Experimental investigation of the overall buckling behaviour of 960MPa high strength steel columns’, *J. Constr. Steel Res.*, vol. 88, pp. 256–266, 2013.
[18] G. Shi, H. Y. Ban, and F. S. K. Bijlaard, ‘Tests and numerical study of ultra-high strength steel columns with end restraints’, *J. Constr. Steel Res.*, vol. 70, pp. 236–247, 2012.
[19] Y. B. Wang, G. Q. Li, S. W. Chen, and F. F. Sun, ‘Experimental and numerical study on the behavior of axially compressed high strength steel box-columns’, *Eng. Struct.*, vol. 58, pp. 79–91, 2014.
[20] Y. B. Wang, G. Q. Li, S. W. Chen, and F. F. Sun, ‘Experimental and numerical study on the behavior of axially compressed high strength steel columns with H-section’, *Eng. Struct.*, vol. 43, pp. 149–159, 2012.

[21] H. Y. Ban, G. Shi, Y. J. Shi, and Y. Q. Wang, 'Overall buckling behavior of 460MPa high strength steel columns: Experimental investigation and design method', *J. Constr. Steel Res.*, vol. 74, pp. 140–150, 2012.

[22] F. Zhou, L. W. Tong, and Y. Y. Chen, 'Experimental and numerical investigations of high strength steel welded h-section columns', *Int. J. Steel Struct.*, vol. 13, no. 2, pp. 209–218, Jul. 2013.

[23] European Committee for Standardization (CEN), *Eurocode 3 - Design of steel structures - Part 1-1: General rules and rules for buildings*. Belgium: Brussels, 2005.

[24] European Committee for Standardization (CEN), *Eurocode 3 - Design of steel structures - Part 1-12 : Additional rules for the extension of EN 1993 up to steel grades S 700*. Belgium: Brussels, 2007.

[25] American Institute of Steel Construction, *Specification for Structural Steel Buildings*. United States: American Institute of Steel Construction, 2016.

[26] Ministry of Construction of the People's Republic of China, *GB 50017-2003. Code for Design of Steel Structures*. Beijing: China Architecture and Building Press, 2003.

[27] T. Y. Ma, Y. F. Hu, X. Liu, G. Q. Li, and K. F. Chung, 'Experimental Investigation into High-strength Q690-steel Welded H-sections under Combined Compression and Bending', *J. Constr. Steel Res.*, vol. 138, pp. 449–462, 2017.

[28] European Committee for Standardization, *BS EN ISO 6892-1:2009. Metallic materials - Tensile testing. Part 1: Method of test at ambient temperature*. Brussels, 2009.

[29] X. Liu and K. F. Chung, 'Experimental investigation into residual stresses of welded H-sections made of Q690 steel materials', in *The 14th East Asia-Pacific Conference on Structural Engineering and Construction*, 2016, pp. 559–565.

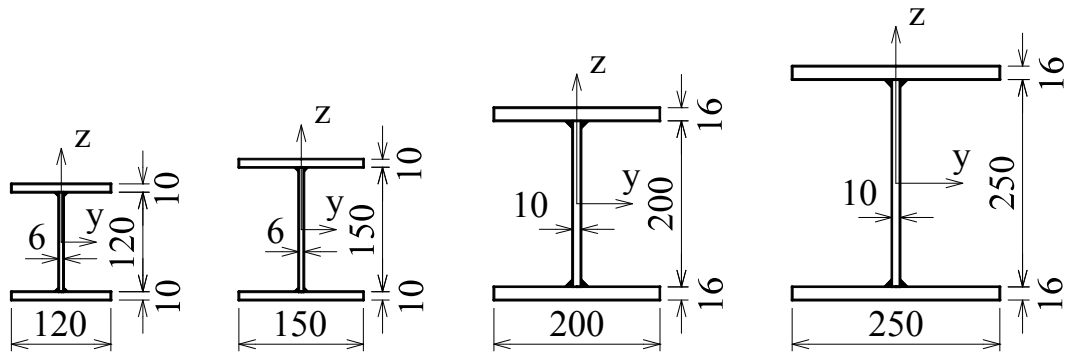

(Class 1) (Class 3) (Class 2) (Class 3)

a) Section H1 b) Section H2 c) Section H3 d) Section H4

Figure 1 Nominal sectional dimensions of slender columns

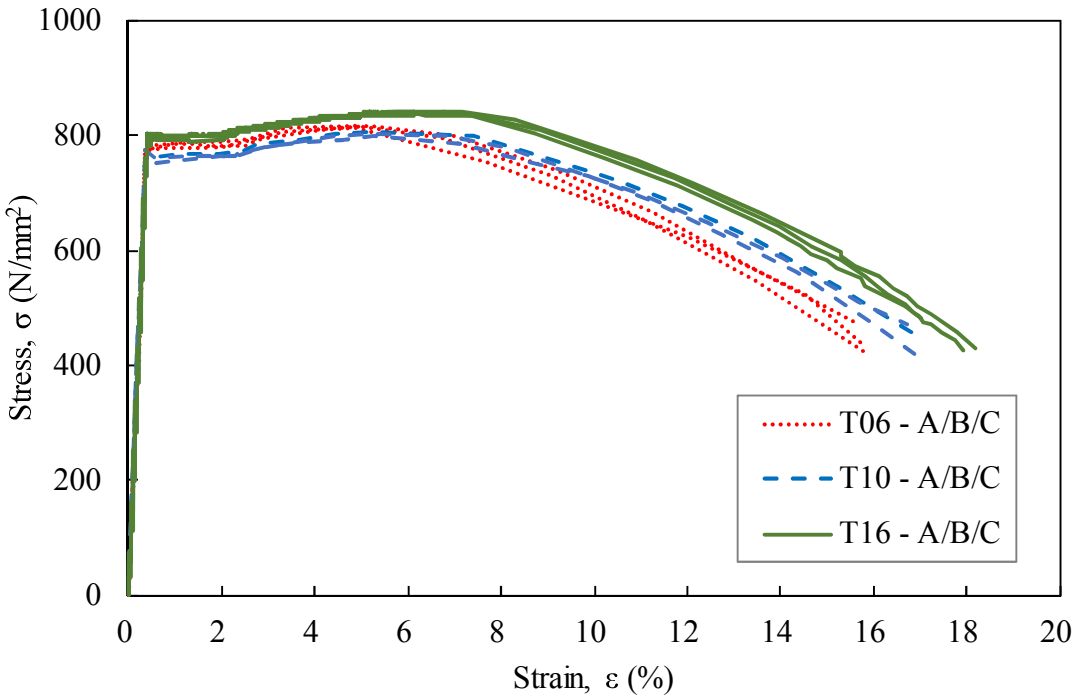

Figure 2 Stress strain curves of various S690 steel plates

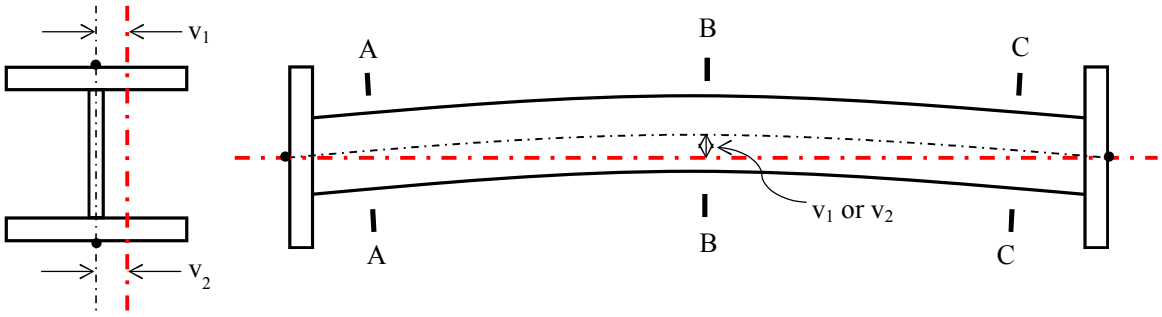

Section B-B

denotes the centreline joining mid-width of the flanges at both ends

- denotes the mid-width of the section flange at mid-length of the section

Figure 3 Measurement method of initial out-of-straightness

Figure 4 Test setup for slender columns under axial compression

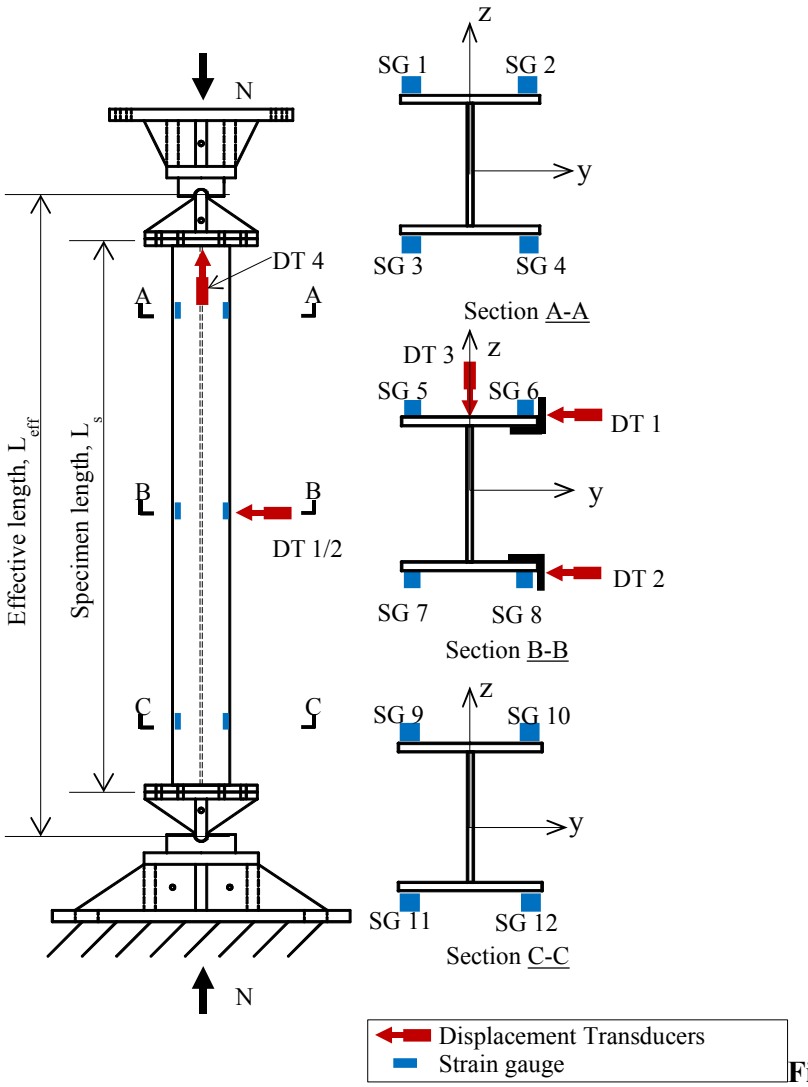

Figure 5Arrangement of strain gauges and displacement transducers

Figure 6 Typical failure mode of slender columns under axial compression

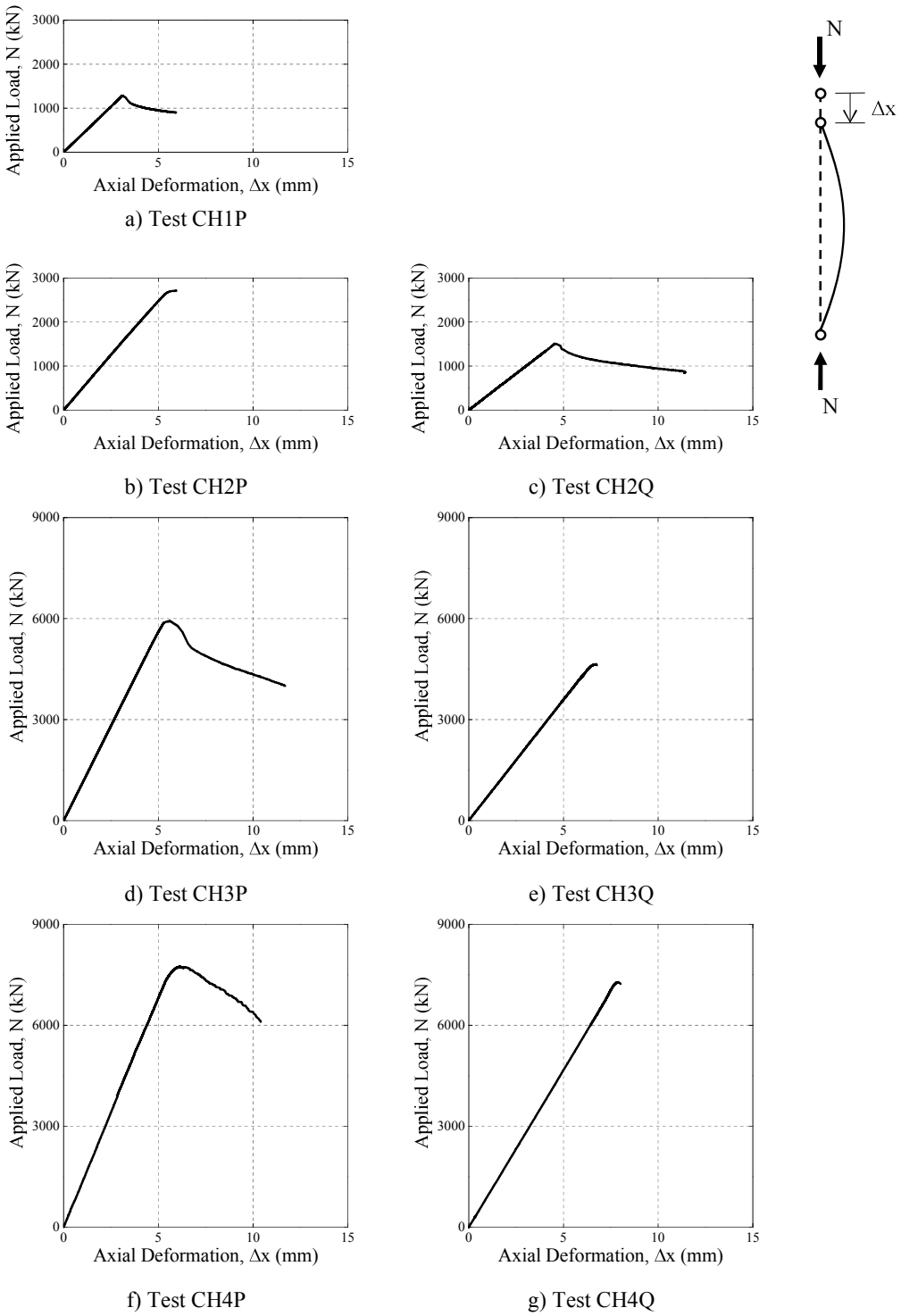

15 **Figure 7 Applied load versus axial deformation curves of slender columns**

16

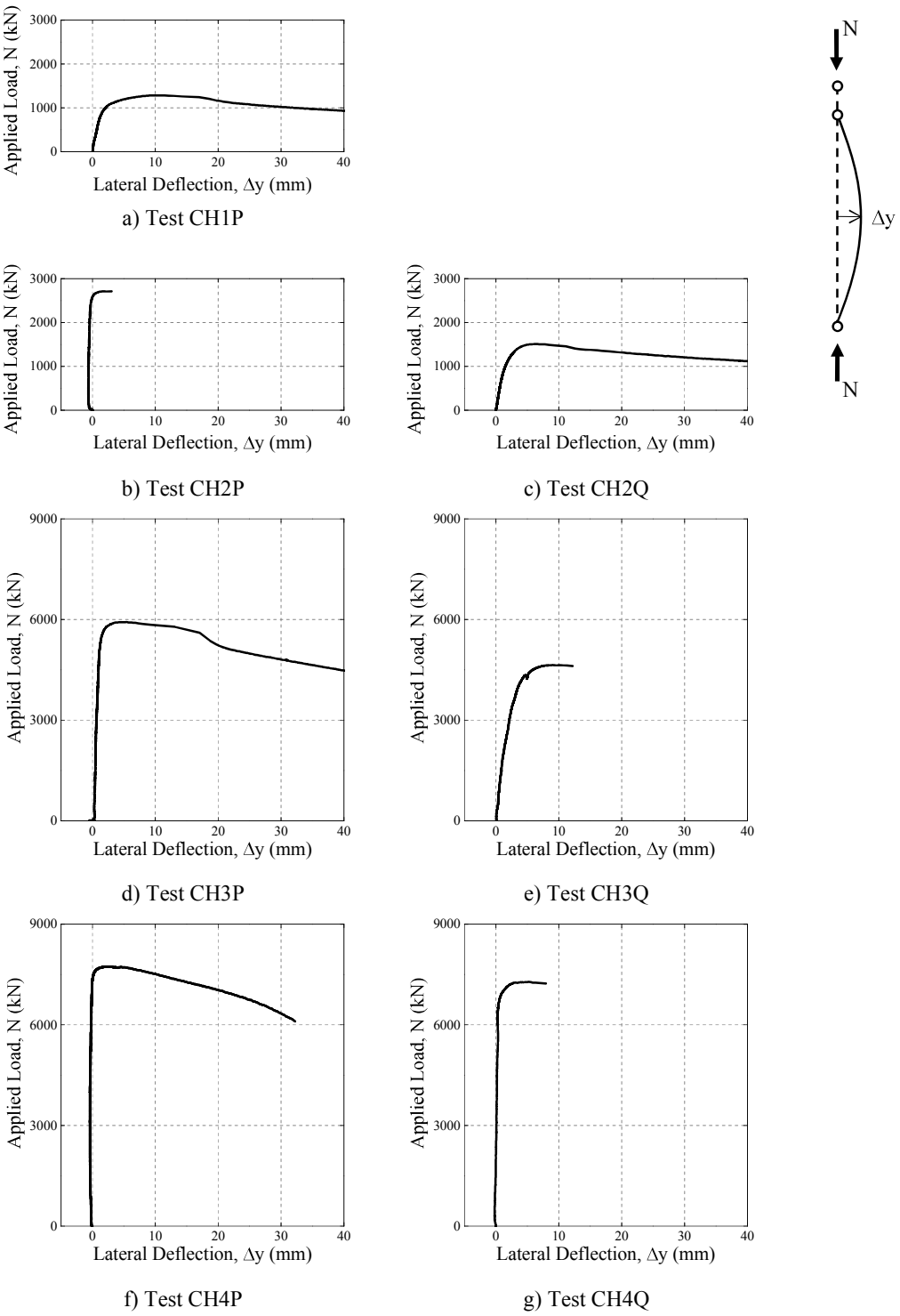

17 **Figure 8 Applied load versus lateral deflection curves of slender columns**

18

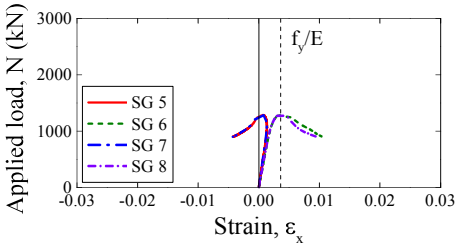

a) Test CH1P

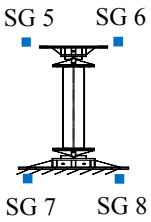

Section B-B

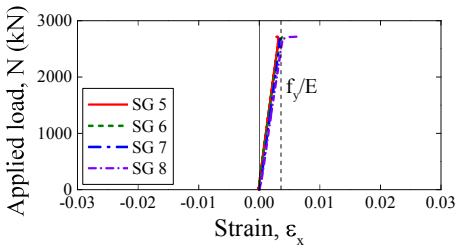

b) Test CH2P

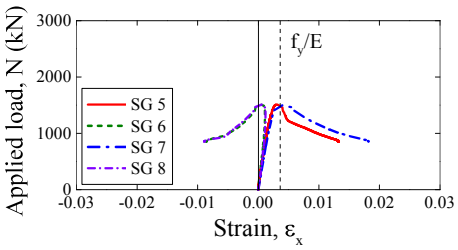

c) Test CH2Q

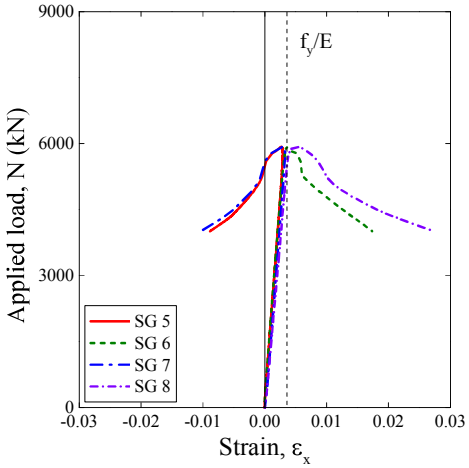

d) Test CH3P

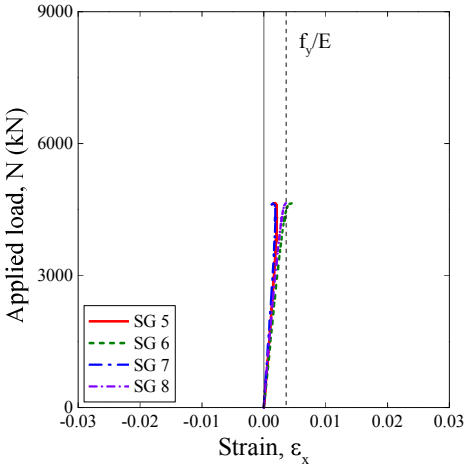

e) Test CH3Q

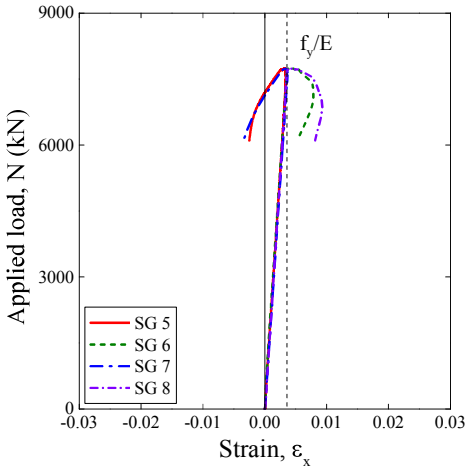

f) Test CH4P

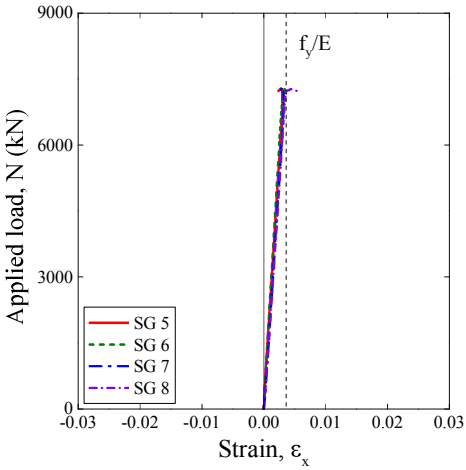

g) Test CH4Q

19 **Figure 9 Applied load versus longitudinal strain curves at mid-height of slender columns**

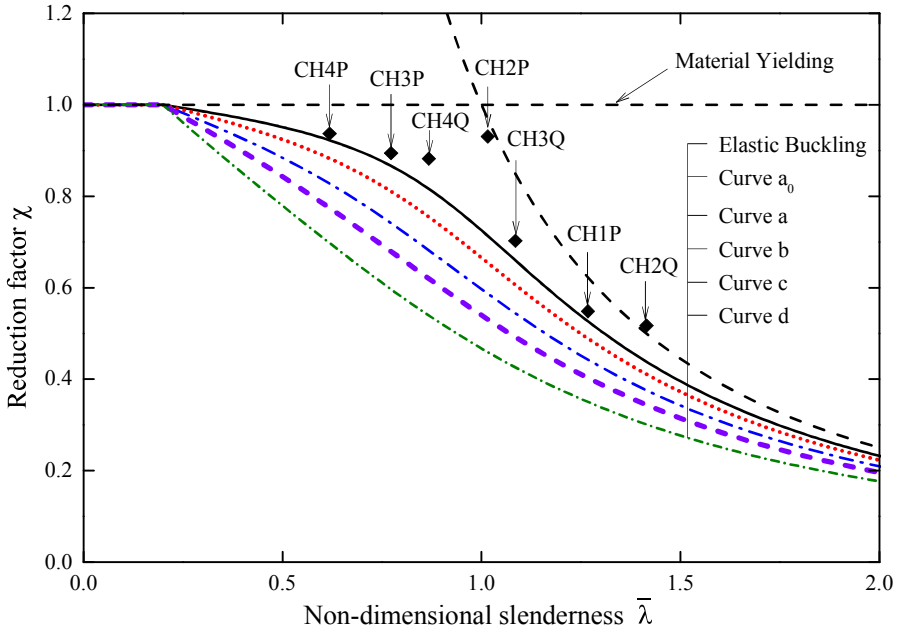

Figure 10 Comparison between measured and predicted resistances of slender columns to EN 1993

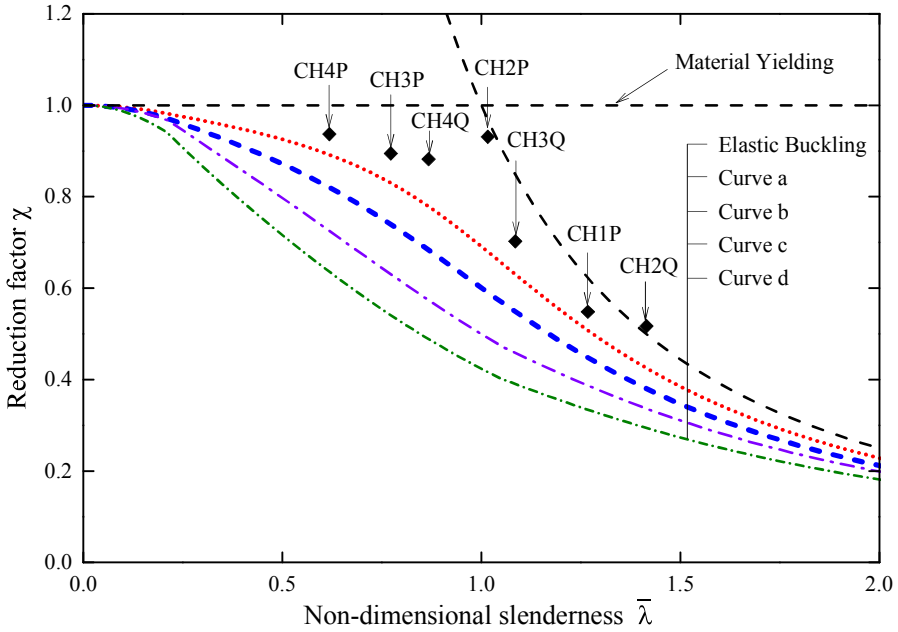

Figure 11 Comparison between measured and predicted resistances of slender columns to GB 50017

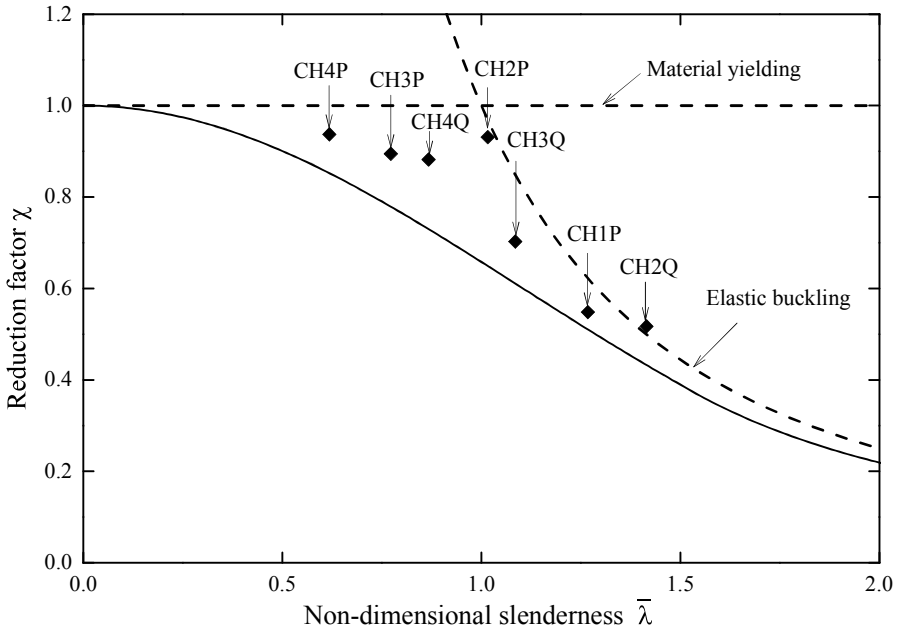

Figure 12 Comparison between measured and predicted resistances of slender columns to ANSI/AISC 360-16

Table 1 Measured dimensions of slender columns

Test	Section Depth h (mm)	Section Width b (mm)	Flange Thickness t_f (mm)	Web Thickness t_w (mm)	Specimen Length L_s (mm)	Effective Length L_{eff} (mm)	Cross sectional Area A (mm^2)	Second moment of area I_z ($\times 10^6$ mm^4)	Radius of Gyration i_z (mm)	λ_z	$\overline{\lambda}_z$
CH1P	141.3	119.6	9.93	5.81	1614.5	1994.5	3079	2.8	30.3	66	1.27
CH2P	170.0	149.0	9.92	5.84	1612.5	1992.5	3833	5.5	37.8	53	1.02
CH2Q	168.4	149.7	9.94	5.83	2414.0	2794.0	3840	5.6	38.0	74	1.41
CH3P	231.2	200.4	16.01	9.93	1616.0	1996.0	8393	21.5	50.6	39	0.77
CH3Q	232.1	200.0	15.98	9.94	2414.0	2794.0	8379	21.3	50.4	55	1.09
CH4P	281.0	250.1	15.99	9.92	1611.5	1991.5	10466	41.7	63.1	32	0.62
CH4Q	281.3	249.8	15.99	9.93	2411.0	2791.0	10465	41.6	63.0	44	0.87

Notes: a) The first character "C" of the designation denotes "Centrically loaded columns".
b) The second and the third characters of the designation denote the sectional designation.
c) The fourth character of the designation denotes different effective lengths of the specimens.

Table 2 Welding parameters for fabrication of S690 steel welded H-sections

Sections	Welding method	Electrode				Welding Parameters				
		Trade mark	Diameter (mm)	Yield strength (N/mm^2)	Tensile strength (N/mm^2)	Voltage (V)	Current (A)	Speed (mm/s)	Fillet size (mm)	Line heat input energy (kJ/mm)
H1, H2	GMAW	CHW-80C1	1.2	660	760	30±1	240±10	4.1±0.5	6	1.76±20%
H3, H4	SAW	CHW-S80	4.0	680	760	36±1	450±15	6.1±0.2	10	2.66±10%

Table 3 Material properties of S690 steel plates

Nominal thickness t (mm)	Coupon	Young's modulus E (kN/mm^2)	Yield strength f_y (N/mm^2)	Tensile strength f_u (N/mm^2)	Ratio f_u/f_y	Elongation at fracture (%)	Strain under tensile strength ε_u	$\varepsilon_u \geq 15 f_y/E$
6	T06-A	210	771	819	1.06	15.5	0.059	Yes
	T06-B	210	764	810	1.06	15.3	0.060	Yes
	T06-C	209	763	817	1.07	16.0	0.058	Yes
	Average	210	766	815	1.06	15.6	0.059	Yes
10	T10-A	212	753	788	1.05	18.2	0.065	Yes
	T10-B	214	758	796	1.05	18.9	0.078	Yes
	T10-C	211	756	794	1.05	18.7	0.067	Yes
	Average	212	756	793	1.05	18.6	0.070	Yes
16	T16-A	208	800	855	1.07	19.7	0.064	Yes
	T16-B	206	797	833	1.05	17.9	0.065	Yes
	T16-C	212	804	843	1.05	19.3	0.068	Yes
	Average	209	800	844	1.05	19.0	0.066	Yes

Table 4 Initial out-of-straightness of slender columns

Test	Initial Out-of-straightness			L_{eff} (mm)	$\lvert v\rvert/L_{eff}$ ($\times 10^{-3}$)
	v_1 (mm)	v_2 (mm)	$v=(v_1+v_2)/2$ (mm)		
CH1P	+0.9	+0.7	+0.8	1994.5	0.4
CH2P	+0.6	--	+0.3	1992.5	0.2
CH2Q	-1.0	-0.9	-1.0	2794.0	0.4
CH3P	+0.6	--	+0.3	1996.0	0.2
CH3Q	-0.7	-0.3	-0.5	2794.0	0.2
CH4P	-0.5	-0.5	-0.5	1991.5	0.3
CH4Q	-0.6	-1.0	-0.8	2791.0	0.3

Notes: a) "+" and "-" indicate positions of initial out-of-straightness on the right and the left of the centerline respectively.
b) "--" indicates a value smaller than 0.25 mm.

Table 5 Failure loads of slender columns

Test	Section Classification	λ_z	$\overline{\lambda}_z$	Failure Mode	N_{test} (kN)
CH1P	1	66	1.27	MB	1284
CH2P	3	53	1.02	MB	2714
CH2Q		74	1.41	MB	1510
CH3P	2	39	0.77	MB	5924
CH3Q		55	1.09	MB	4644
CH4P	3	32	0.62	MB	7739
CH4Q		44	0.87	MB	7284

Note: "MB" denotes member buckling.

Table 6 Imperfection factors for buckling design to EN 1993-1-1

Buckling curve	a_0	a	b	c	d
Imperfection factor α	0.13	0.21	0.34	0.49	0.76

Table 7 Comparison on buckling resistances for slender columns to EN 1993-1-1

Test	λ	$\bar{\lambda}$	N_{test} (kN)	$N_{c,Rd}$ (kN)	$\chi_t = \frac{N_{test}}{N_{c,Rd}}$	$\chi_{EC3,c}$	$\frac{\chi_t}{\chi_{EC3,c}}$	$\chi_{EC3,a0}$	$\frac{\chi_t}{\chi_{EC3,a0}}$
CH1P	66	1.27	1284	2342	0.55	0.40	1.38	0.53	1.04
CH2P	53	1.02	2714	2915	0.93	0.53	1.75	0.71	1.31
CH2Q	73	1.41	1510	2920	0.52	0.35	1.49	0.44	1.18
CH3P	39	0.77	5924	6623	0.89	0.68	1.31	0.87	1.03
CH3Q	55	1.09	4644	6611	0.70	0.49	1.43	0.66	1.06
CH4P	32	0.62	7739	8259	0.94	0.77	1.22	0.92	1.02
CH4Q	44	0.87	7284	8257	0.88	0.62	1.42	0.82	1.08

Table 8 Imperfection factors for buckling design to GB 50017-2003

Buckling curve		a	b	c		d	
				$\bar{\lambda} \le 1.05$	$\bar{\lambda} > 1.05$	$\bar{\lambda} \le 1.05$	$\bar{\lambda} > 1.05$
Imperfection Factors	α_1	0.410	0.650	0.730		1.350	
	α_2	0.986	0.965	0.906	1.216	0.868	1.375
	α_3	0.152	0.300	0.595	0.302	0.915	0.432

Table 9 Comparison on buckling resistances for slender columns to GB 50017

Test	λ	$\bar{\lambda}$	N_{test} (kN)	$A_f f_{y,f}+A_w f_{y,w}$ (kN)	$\chi_t = \frac{N_{test}}{A_f f_{y,f} + A_w f_{y,w}}$	$\chi_{GB,b}$	$\frac{\chi_t}{\chi_{GB,b}}$	$\chi_{GB,a}$	$\frac{\chi_t}{\chi_{GB,a}}$
CH1P	66	1.27	1284	2342	0.55	0.45	1.22	0.51	1.08
CH2P	53	1.02	2714	2915	0.93	0.59	1.57	0.68	1.37
CH2Q	73	1.41	1510	2920	0.52	0.38	1.36	0.43	1.22
CH3P	39	0.77	5924	6623	0.89	0.74	1.20	0.83	1.07
CH3Q	55	1.09	4644	6611	0.70	0.55	1.28	0.63	1.11
CH4P	32	0.62	7739	8259	0.94	0.82	1.15	0.89	1.05
CH4Q	44	0.87	7284	8257	0.88	0.68	1.29	0.78	1.13

Table 10 Comparison on buckling resistances for slender columns to ANSI/AISC 360-16

Test	λ	$\bar{\lambda}$	N_{test} (kN)	$A_f f_{y,f}+A_w f_{y,w}$ (kN)	$\chi_{test} = \frac{N_{test}}{A_f f_{y,f} + A_w f_{y,w}}$	χ_{ANSI}	$\frac{\chi_{test}}{\chi_{ANSI}}$
CH1P	66	1.27	1284	2342	0.55	0.51	1.08
CH2P	53	1.02	2714	2915	0.93	0.65	1.43
CH2Q	73	1.41	1510	2920	0.52	0.44	1.18
CH3P	39	0.77	5924	6623	0.89	0.78	1.15
CH3Q	55	1.09	4644	6611	0.70	0.61	1.15
CH4P	32	0.62	7739	8259	0.94	0.85	1.10
CH4Q	44	0.87	7284	8257	0.88	0.73	1.21